Chapter 7

Magnetic reconnection

During periods of southward IMF magnetic reconnection connects closed geomagnetic field with interplanetary magnetic field generating newly opened magnetic flux (Figure 8.1). Along the newly opened field particles can freely enter and leave the magnetosphere. The newly opened field is swept with the solar wind along the magnetosphere and magnetic flux accumulates at the tail boundary. The accumulation of magnetic flux in the magnetotail lopes increases the size of the tail magnetosphere and magnetic energy is stored in the lobes of the magnetotail. Thus reconnection at the dayside magnetopause is important for the energy budget of the entire magnetosphere. The subsequent processes in the magnetotail will be addresses in the section on the magnetotail.

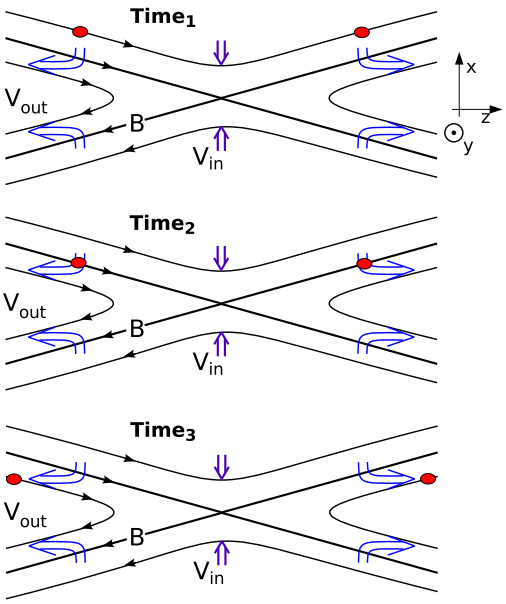

Figure 7.1: Sketch of the magnetic reconnection geometry and the associated plasma and magnetic flux transport.

7.1 General Properties and Definition

Magnetic reconnection implies a new connection of magnetic flux (or field lines) and therefore requires a violation of Ohm's law albeit in a very small region. Figure 7.1 illustrates the basic geometry

and how magnetic flux and plasma is transported in a reconnection process. The thicker plotted magnetic field lines that cross in the center are called separatrices and the point where they cross is called an X-point or X-line (when the 3D aspect is emphasized). The blue arrows indicate qualitatively the plasma flow. The regions above and below the separatrices are called the inflow regions and the regions to the left and right are called the outflow regions. Although not required it can in general be assumed that the region at sufficient distance from the X line is ideal, i.e., that the frozen-in condition (Chapter 2) is satisfied.

The two red spots in the figure indicate plasma elements which are assumed to be at sufficient distance from the X-line such that the frozen-in condition applies to these elements. At time 1 both elements are connected by the same field line. At time 2 they are convected to the position of the X-line which implies that the magnetic field line on which they are located is now the new separatrix. At time 3 these elements are now in the outflow region and are located clearly on two separate magnetic field lines. Here the key property is the transport of the plasma elements from one side of the reconnection geometry (inflow region) across the separatrix into the outflow regions. This property can be used to identify or define magnetic reconnection:

Definition: Magnetic reconnection is a process in which plasma is transported across a separatrix surface.

It is important to note that this transport across a separatrix implies the violation of the frozen-in condition because plasma elements, which were originally connected by a field line, are later found on separate field lines. However, as mentioned this violation of the frozen-in condition is not required at the locations of the plasma elements but only in a small vicinity of the X-line (in fact strictly it would be sufficient to have a violation of the frozen-in condition only at the X-line, although this is somewhat singular). To illustrate this point let us consider a representation of the two-dimensional magnetic field (in the x, z plane) by the y component of the vector potential $\mathbf{B} = \nabla A_y \times \mathbf{e}_y$ which implies $B_z = \partial A_y/\partial x$ and $B_x = -\partial A_y/\partial z$. For $B_z > 0$ for $z > 0$ (assumed in Figure 7.1) this implies that A_y has a local minimum at the X-line in a cut along x and a local maximum in a cut along z. In other words the X-point represents a saddle point for the vector potential A_y. Assuming a simple form of Ohm's law

$$\mathbf{E} = -\mathbf{u} \times \mathbf{B} + \eta \mathbf{j}$$

where the resistivity is nonzero only in the vicinity of the X-line. Using the vector potential the $y$component of Ohm's law can be written as

$$\frac{dA_y}{dt} = \frac{\partial A_y}{\partial t} + \mathbf{u} \cdot \nabla A_y = -\eta j_y$$

Noting that the current density at the X-line is negative $r = -\eta j_y|_{xl} > 0$ such that the change of the vector potential at the X-line is

$$\left.\frac{dA_y}{dt}\right|_{xl} = E_{y,xl} = r$$

Since this defines the separatrix, the value of A_y of the separatrix is increasing in time at a rate of r. Since $A_y$increases with x this implies field lines that have been originally in the inflow region will

eventually become separatrices. Note also for fluid elements in the ideal plasma region Ohm's law implies

$$\frac{dA_y}{dt} = \frac{\partial A_y}{\partial t} + \mathbf{u} \cdot \nabla A_y = 0$$

in other words the value of the vector potential for the fluid element does not change along its path, i.e., $A_{y,fl} = \text{const}$. Thus if a fluid element is located at time 1 in the inflow region on a field line with $A_{y,fl} > A_{y,xl}$ at some later time 2 the A_y value of the X-line/separatrix will have increased to the value of $A_{y,fl}$ such that the plasma element is now located on the separatrix. As time continues $A_{y,xl}$ increases further such that the fluid element will be found in the outflow region.

Let us finally remark that this use of the vector potential is a straightforward measure of the magnetic flux in the two-dimensional plane, i.e., the amount of magnetic flux between two points $\mathbf{r}_a$ and $\mathbf{r}_b$ (assuming a unit length along the invariant direction y) is just the difference $\Phi_{ab} = A_y(\mathbf{r}_b) - A_y(\mathbf{r}_a)$. Hence the change of $A_{y,xl}$ is a direct measure of the amount of magnetic flux that is moved from the inflow region into the outflow region. The rate of the flux magnetic transport $r = -\eta j_y|_{xl}$ is called the reconnection rate.

Alternative definition: The 2D example illustrates that reconnection can also be identified/defined by the violation of the frozen-in condition at a X-line.

Finally it ought to be mentioned that there is considerable work on three-dimensional reconnection and associated concepts. A simple extension of the prior example which provides a little insight into 3D aspects is the assumption of a magnetic field into the plane (y direction). Note that the system still remains two-dimensional unless there is an actual variation along the y direction. A magnetic field would along y has almost no influence on the dynamics (it can be treated as an additional pressure term). The resulting geometry is more generic then the highly idealized case of strictly anti-parallel fields in our example which is singular in terms of actual applications. Since the dynamics in the x, z plane does not change everything in our discussion of reconnection remains valid applicable including the interpretation of the reconnection rate. However, with a B_y component the electric field at the X line is now along B_y whereas before this was a magnetic neutral line. From Ohm's law we know that the component of the electric field along the magnetic field must be 0 in an ideal plasma and thus there is a parallel electric field only in the vicinity of the X-line.

2nd alternative definition: We can use this property to postulate that three-dimensional magnetic reconnection is equivalent to the presence of an electric field parallel to the magnetic field in a sufficiently small region of space.

Note that this is a nontrivial property because $E_\parallel = \mathbf{E} \cdot \mathbf{B}/B$ is usually 0 in space plasma. This provides also a physically sound definition in the sense that $\mathbf{E} \cdot \mathbf{B}$ is a Lorentz invariant, i.e., the identification or definition of reconnection using this property is independent of the frame of reference. There are many more interesting aspects of reconnection in three dimensions which can found in the literature ... but for the purpose of this text it seems more important to discuss the actual dynamics of the more classical models of magnetic reconnection.

7.2 Magnetic Diffusion and Lundquist Number

In terms of analytic theory there are two main analytic approaches to the process of magnetic reconnection. One uses a steady state assumption for the local reconnection geometry and the other one

treats reconnection as an instability (tearing mode) and addresses questions like the onset of reconnection. This instability aspect is more relevant for magnetotail dynamics.

Lundquist (or magnetic Reynolds number):

Ohm's law is of central importance for magnetic reconnection. In Chapter 2 we introduced general Ohm's law as

$$\mathbf{E}+\mathbf{u}\times\mathbf{B}=\frac{m_e m_i}{e^2\rho}\left[\frac{\partial\mathbf{j}}{\partial t}+\nabla\cdot(\mathbf{uj}+\mathbf{ju})\right]-\frac{M}{e\rho}\nabla\underline{\underline{\mathbf{p}}}_e+\frac{m_i}{e\rho}\mathbf{j}\times\mathbf{B}+\eta\mathbf{j} \tag{7.1}$$

with the resistivity $\eta = m_e\nu_c/ne^2$ where ν_c is the collision frequency between electrons and ions (or neutrals). Starting from general Ohm's Law this discussion focuses on the terms that can support an Electric field in the absence of plasma flow.

Lundquist number

Resistive Ohm's law:

$$\mathbf{E}=-\mathbf{u}\times\mathbf{B}+\eta\mathbf{j}$$

Using Ampere's law and the induction equation

$$\frac{\partial\mathbf{B}}{\partial t}=-\nabla\times\mathbf{E}=\nabla\times(\mathbf{u}\times\mathbf{B}-\eta\mathbf{j})$$

and for constant resistivity and assuming $\mathbf{u}=0$:

$$\frac{\partial\mathbf{B}}{\partial t}=-\frac{\eta}{\mu_0}\nabla\times\nabla\times\mathbf{B}=\frac{\eta}{\mu_0}\Delta\mathbf{B} \tag{7.2}$$

Diffusion equation for magnetic field. The solution for specific initial/boundary conditions can be found easily through separation of variables. For the special case of a force free magnetic field

$$\mu_0\mathbf{j}=\nabla\times\mathbf{B}=\alpha\mathbf{B}$$

with $\alpha = \text{const} = 1/L$ equation 7.2 reduces to

$$\frac{\partial\mathbf{B}}{\partial t}=\frac{\eta}{\mu_0}\Delta\mathbf{B}=-\frac{\eta}{\mu_0}\alpha^2\mathbf{B}$$

with the solution

$$\begin{aligned}\mathbf{B}(\mathbf{r},t) &= \mathbf{B}(\mathbf{r},0)\exp\left(-\frac{\eta t}{\mu_0 L^2}\right)=\mathbf{B}(\mathbf{r},0)\exp\left(-\frac{t}{\tau_{diff}}\right)\\ \text{with}\qquad \tau_{diff}&=\frac{\mu_0 L^2}{\eta}\end{aligned}$$

Normalization of 7.2 to identify typical diffusion time scale τ_{diff} using a typical system gradient length scale L yields the same result for τ_{diff}. Note that this is independent of the normalization of the magnetic field. Also since diffusion requires the presence of a current L can be interpreted as a typical current width (or half-width). This also allows to identify a velocity which corresponds to diffusion as $v_{diff} = L/\tau_{diff} = \eta/(\mu_0 L)$.

Another way to look at the problem of diffusion is to examine the distance a line of force can slip through the plasma in a given time τ. Using the above result this distance is

$$l_{diff} = \sqrt{\frac{\eta\tau}{\mu_0}}$$

We would like to set these diffusion properties (time and velocity) in relation to other typical time scales and velocities. In Chapter 2 we used a normalization that is based on the Alfven speed $v_A = B_0/\sqrt{\mu_0\rho_0}$ and $\tau_A = L/v_A$. In fact when we use the Alfven speed and time for the normalization we obtain for the normalized Ohm's law

$$\widetilde{\mathbf{E}} = -\widetilde{\mathbf{u}} \times \widetilde{\mathbf{B}} + \widetilde{\eta}\widetilde{\mathbf{j}}$$

where $j_0 = B_0/(\mu_0 L)$ and $\widetilde{\eta} = \eta\tau_A/(\mu_0 L^2) = \tau_A/\tau_{diff}$. Another way to express this is in terms of the so-called Lundquist number

$$R = \frac{\tau_{diff}}{\tau_A} = \frac{1}{\widetilde{\eta}} = \frac{\mu_0 L^2}{\eta\tau_A} = \frac{\mu_0 L v_A}{\eta}$$

In a typical space plasma $R \gg 1$, i.e., diffusion is an incredibly slow process. Using the resistivity$\eta = m_e\nu_c/ne^2$and the definition of the electron skin depth the normalized resistivity becomes $\widetilde{\eta} = 1/R = \lambda_e^2\nu_c\tau_A/L_0^2$ and $\tau_{diff} = L_0^2/(\lambda_e^2\nu_c)$. Using typical values for the magnetopause, the near Earth magnetotail, and for the solar corona (for comparison) we obtain the following table which summarizes the basic plasma parameters and gives values for the collision frequency, the electron skin depth, the diffusion time, and the Lundquist number.

	Magnetopause	Magnetotail	Solar corona (flares)
n_0 [cm^{-3}]	4	0.5	$6 \cdot 10^8$
B_0 [nT]	40	20	$3 \cdot 10^7$
L_0 [m]	10^6	10^7	10^7
v_A [m/s]	$4.4 \cdot 10^5$	$6.2 \cdot 10^5$	$2.7 \cdot 10^7$
τ_A $[s]$	2.3	1.6	0.37
T_i $[K]$	10^6	$5 \cdot 10^7$	10^6
T_e $[K]$	10^5	$5 \cdot 10^6$	10^6
ω_{pe} [s^{-1}]	$1.1 \cdot 10^5$	$4.0 \cdot 10^4$	$1.4 \cdot 10^9$
Λ	$1.3 \cdot 10^{11}$	$1.3 \cdot 10^{13}$	$7 \cdot 10^7$
ν_c [s^{-1}]	$2 \cdot 10^{-7}$	10^{-9}	10
λ_e [m]	$2.7 \cdot 10^3$	$8.0 \cdot 10^3$	0.2
τ_{diff} $[s]$	$7 \cdot 10^{11}$	$1.5 \cdot 10^{15}$	$2.5 \cdot 10^{14}$
R	$3 \cdot 10^{11}$	10^{15}	10^{15}

The values demonstrate that in all three systems the Lundquist number is very large with a correspondingly large value for the diffusion time. Note that this is strictly not correct for the magnetopause and the magnetotail because the collision time $\tau_c = 1/\nu_{ei} \approx 10^7 - 10^9$s is much longer than the time a particle would spend at the magnetopause or in the magnetosheath.

7.3 Sweet-Parker Reconnection

This model has first been suggested by *Sweet* [1958] and independently by *Parker* [1957] and is based on a discussion of the pressure balance in the region of reconnection. In addition the model uses a classical resistivity (which can be substituted by other types of resistive interaction). The basic geometry is illustrated in Figure 7.2.

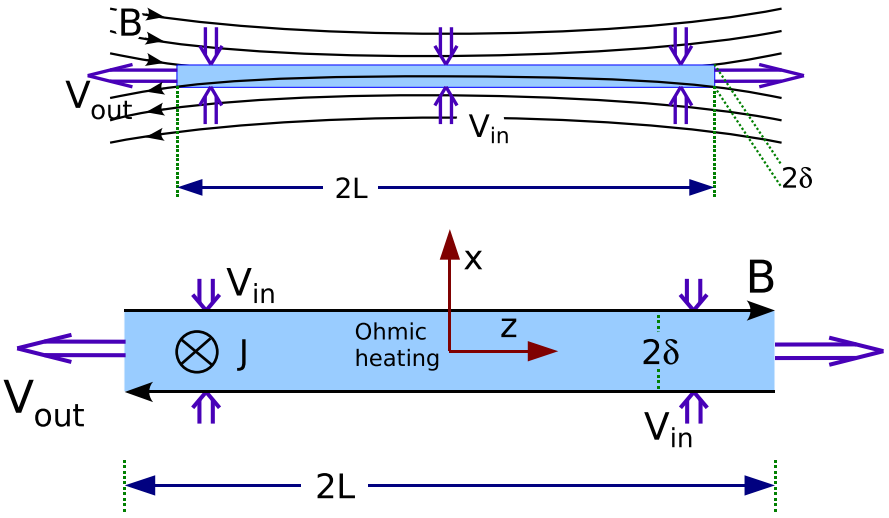

Figure 7.2: Illustration of the Sweet-Parker reconnection geometry. The top plot shows the overall geometry and the bottom plot illustrates the diffusion region.

The basic boundary conditions of this geometry are relatively straightforward. We assume that the diffusion region has a total length of L and total thickness of 2δ. At the inflow region we consider a magnetic field B_0 that is strongly tangential to the inflow boundary. The inflow velocity is approximately constant with a value of v_{in}. At the outflow boundary the magnetic field is B_{out} and the the outflow velocity is v_{out}. Note the the region inside the diffusion region is assumed to be dominated by diffusion where the outside region is assumed to be ideal. Other properties can be inferred from basic plasma physics. Total pressure balance $B^2/(2\mu_0) + p = \text{const}$ between the center of the diffusion region ($x = 0$) where the magnetic field is 0 and the inflow boundary implies

$$p_c - p_{in} = \frac{B_0^2}{2\mu_0}$$

Since the plasma is accelerated outward through $\mathbf{j} \times \mathbf{B}$ force the plasma velocity at the outflow boundary is

$$v_{out} = v_A = \frac{B_0}{\sqrt{\mu_0 \rho_{out}}}$$

Let us now consider the pressure equation for an MHD fluid (chapter 2)

$$\frac{1}{\gamma-1}\left(\frac{\partial p}{\partial t}+\nabla\cdot p\mathbf{u}\right)=-p\nabla\cdot\mathbf{u}+\eta\mathbf{j}^2$$

$$\frac{dp}{dt}=\frac{\partial p}{\partial t}+\mathbf{u}\cdot\nabla p=-\gamma p\nabla\cdot\mathbf{u}+(\gamma-1)\,\eta\mathbf{j}^2$$

Considering that (a) the dominant transport is along the current sheet (in the z direction), (b) the velocity increases linearly from 0 at the center to v_A at the outflow boundary, and (c) the current density is given by $j_0 = B_0/(\mu_0\delta)$ we can write the pressure equation for the central point of the diffusion region (where $u = 0$) as

$$\begin{aligned}\frac{\partial p_c}{\partial t} &= -\gamma p_c\nabla\cdot\mathbf{u}+(\gamma-1)\,\eta\mathbf{j}^2\\ &= -\gamma p_c\frac{\Delta u_z}{L}+(\gamma-1)\,\eta\frac{B_0^2}{\mu_0^2\delta^2}\\ &= -\gamma\left(\frac{B_0^2}{2\mu_0}+p_{in}\right)\frac{v_A}{L}+(\gamma-1)\,\eta\frac{B_0^2}{\mu_0^2\delta^2}\end{aligned}$$

Assuming a steady pressure in the center of the diffusion region and $p_{in} = \lambda B^2/(2\mu_0)$ leads to

$$\frac{v_A}{L}=\frac{2\,(\gamma-1)}{\gamma\,(1+\lambda)}\frac{\eta}{\mu_0\delta^2}$$

or

$$\delta=\sqrt{\frac{2\,(\gamma-1)}{\gamma\,(1+\lambda)}\frac{\eta L}{\mu_0 v_A}}=\sqrt{\frac{2\,(\gamma-1)}{\gamma\,(1+\lambda)}}\frac{L}{\sqrt{R}}$$

with the Lundquist number $R = \mu_0 L v_A/\eta$ based on the length scale L. A relation for the inflow and outflow velocities can be obtained from the continuity equation (using constant density) by noting that the flux into the diffusion region must balance the flux out of the diffusion region

$$v_{in}L=v_A\delta\quad\text{or}\quad v_{in}=v_A\frac{\delta}{L}\approx v_A/\sqrt{R}$$

The resulting reconnection rate for the Sweet parker model is

$$E_{xl}=\eta j_{xl}=\eta\frac{B_0}{\mu_0\delta}=\frac{B_0 L v_A}{R\delta}\approx\frac{B_0 v_A}{\sqrt{R}}$$

Thus the reconnection rate normalized to the typical electric field $E_0 = B_0 v_A$ is

$$r = \frac{v_{in}}{v_A} \simeq \frac{1}{\sqrt{R}}$$

Magnetic flux conservation can also be used to determine the magnetic field at the outflow boundary according to

$$v_{in}B_0 = v_A B_{out} \quad \text{or} \quad B_{out} = B_0 \frac{v_{in}}{v_A} = B_0/\sqrt{R}$$

Since the Lundquist or magnetic Reynolds number is typically a very large number, the resulting reconnection rate is very small. This implies also a very large aspect ratio L/δ. Note, however, that this still depends on the length scale L which is not necessarily fixed in this approach.

Is the time $\tau_A = L/v_A$ sufficient for magnetic field to diffuse of the distance δ? Using the diffusion length the diffusion length is

$$l_{diff} = \sqrt{\frac{\eta\tau_A}{\mu_0}} = \sqrt{\frac{\eta L}{\mu_0 v_A}} = \frac{L}{\sqrt{R}} = \delta,$$

i.e., consistent with the width of the diffusion region. The basic physics assumed in this model is relatively simple. The aspect ratio of the diffusion region is mostly fixed by the assumption of Ohmic heating ηj^2 and the required flow to maintain a constant pressure at the center of the diffusion region. If the diffusion region were wider compared to L the heating would be too small to sustain the flow. If it were narrower the heating would be too rapid resulting in an excess pressure violating the pressure balance requirement.

It should be noted that this is not a self-consistent treatment of the reconnection problem or the diffusion region. The derived relations use a number of assumption and estimates most of which are straightforward such as pressure balance etc. However, other assumptions are not straightforward such as the constancy of the density, the precise flow profile, or the assumed length of the diffusion region L. While there may be geometrical arguments for a certain scale L the system could in principle realize a much smaller length L. For smaller L the Lundquist number becomes smaller $\sim L$ with a resulting larger reconnection rate. To illustrate this point let us assume that the length of the diffusion region is indeed $L_1 \ll L$. This particularly implies that

$$\begin{aligned} R_1 &= \mu_0 L_1 v_A/\eta = \frac{L_1}{L} R \\ r_1 &= \frac{\delta_1}{L_1} = \frac{v'_{in,1}}{v_A} \simeq \frac{1}{\sqrt{R_1}} = \sqrt{\frac{L}{L_1}} r \\ \delta_1 &= \sqrt{\frac{L_1}{L}} \delta \end{aligned}$$

This illustrates that the reconnection rate can be much higher if the system is able to realize a much shorter diffusion region. This idea is central in Petschek's reconnection model where a small diffusion region is imbeeded in the much larger system as illustrated later.

Alternative derivation: Consider Electric field in the inflow region $E_{in} = v_{in}B_0$ and electric field at the X-line $E_{xl} = \eta j_{xl} = \frac{\eta B_0}{\mu_0 \delta}$. With $E_{in} = E_{xl}$ we obtain

$$v_{in} = \frac{\delta}{\tau_{diff}} = \frac{\eta}{\mu_0 \delta}$$

which is the same as the diffusion velocity v_{diff} derived before. Using $\tau_{diff} = \mu_0 \delta^2/\eta$ and flux conservation $L v_{in} = \delta v_{out}$ we can eliminate δ from the above equation

$$v_{in}^2 = \frac{\eta v_{out}}{\mu_0 L}$$

With $R = \mu_0 L v_A/\eta$ we obtain

$$v_{in}^2 = \frac{v_{out} v_A}{R}$$

or

$$r = M_{in} = \frac{v_{in}}{v_A} = \frac{\sqrt{v_{out}/v_A}}{\sqrt{R}}$$

where r is the dimensionless reconnection rate which is equal to the inflow Alfven Mach number M_{in}. From density and magnetic flux conservation we obtain:

$$\begin{aligned} \delta &= L\frac{v_{in}}{v_{out}} \\ B_{out} &= B_0\frac{v_{in}}{v_{out}} \end{aligned}$$

Now we have almost the same relations as in the prior derivation except for a specification of the outflow speed. To obtain the outflow speed let us consider the force balance along the z direction in steady state by assuming acceleration from $\mathbf{j} \times \mathbf{B}$ forces, i.e., $\rho \mathbf{u} \cdot \nabla \mathbf{u} = \mathbf{j} \times \mathbf{B}$ or

$$\rho \frac{v_{out}^2}{L} \approx \frac{B_0 B_{out}}{\mu_0 \delta}$$

From flux conservation or $\nabla \cdot \mathbf{B} = 0$ we get $B_{out}/\delta = B_0/L$ such that

$$v_{out} = \frac{B_0}{\sqrt{\mu_0 \rho}} = v_A$$

This yields the previous result for the reconnection flow and the aspect ratio:

$$v_{in} = \frac{v_A}{\sqrt{R}} \quad \text{and} \quad \frac{\delta}{L} = \frac{1}{\sqrt{R}}$$

This derivation did not make use of the pressure equation at all. Therefore it appears that the result is fairly robust and reflects more a scaling law rather than a concise treatment of the diffusion region. In fact, there is at present no self-consistent analytic solution for the diffusion region even though there have been many attempts. One complication is is illustrated considering the continuity and the pressure equations

$$\begin{aligned} \frac{\partial \rho}{\partial t} &= -\mathbf{u}\cdot\nabla\rho - \rho\nabla\cdot\mathbf{u} \\ \frac{\partial p}{\partial t} &= -\mathbf{u}\cdot\nabla p - \gamma p\nabla\cdot\mathbf{u} + (\gamma-1)\,\eta\mathbf{j}^2 \end{aligned}$$

Assuming a steady state solution at the stagnation point (X=line) where $\mathbf{u}=0$ yields

$$\begin{aligned} 0 &= -\rho\nabla\cdot\mathbf{u} \\ 0 &= -\gamma p\nabla\cdot\mathbf{u} + (\gamma-1)\,\eta\mathbf{j}^2 \end{aligned}$$

Thus the continuity equation implies either $\rho=0$ which is unphysical or $\nabla\cdot\mathbf{u}=0$ at the X-line. However, the latter choice leads to $(\gamma-1)\,\eta\mathbf{j}^2=0$. This implies either $\eta j^2=0$ which is not acceptable because it would imply that there is no electric field thereby contradicting the notion of reconnection; or it implies $\gamma=1$ which means an isothermal system. This could be realized for instance by large thermal conductivity. Actually assuming a steady pressure makes sense because the pressure is forced to balance the magnetic pressure outside the diffusion region. This implies $\nabla\cdot\mathbf{u}=(\gamma-1)\,\eta\mathbf{j}^2/(\gamma p)$ at the X-line. using the result for the continuity equation at the X-line yields

$$\frac{1}{\rho_{xl}}\frac{\partial\rho_{xl}}{\partial t} = -\left.\frac{(\gamma-1)\,\eta\mathbf{j}^2}{\gamma p}\right|_{xl}$$

with the solution

$$\begin{aligned} \rho_{xl}(t) &= \rho_{0,xl}\exp\left(-t/\tau_\rho\right) \\ with \qquad \tau_\rho &= \left.\frac{\gamma p}{(\gamma-1)\,\eta\mathbf{j}^2}\right|_{xl} \simeq \frac{\gamma B_0^2}{2\,(\gamma-1)\,\mu_0 E_{xl} j_{xl}} = \frac{\gamma L}{2\,(\gamma-1)\,v_A} = \frac{\gamma}{2\,(\gamma-1)}\tau_{A,L} \end{aligned}$$

where the τ_ρ been derived using the prior relations and the definition of the Lundquist number. Various attempts to model steady reconnection use incompressible dynamics which eliminates the pressure equation through the condition $\nabla\cdot\mathbf{u}=0$. Formally this can be seen by the fact that the pressure contribution goes to 0 for $\gamma\to\infty$ in the total energy density (equation 6.17). This example demonstrates that a stationary solution may not be possible in the framework of the compressible MHD without either singularity at the X-line or without considering a heat flux or special values for γ.

7.4 Petschek Reconnection

As noted in the preceding section the long aspect ratio limits the possible reconnection rate in the Sweet-Parker model. *Petschek* [1964] realized that a much larger reconnection rate would be possible if the diffusion region were much shorter. In fact, as noted earlier the diffusion electric field needs to be present only in a very small vicinity of the X-line. A long and narrow diffusion region implies that all flow must go through the narrow channels as illustrated for the flux of mass and magnetic field.

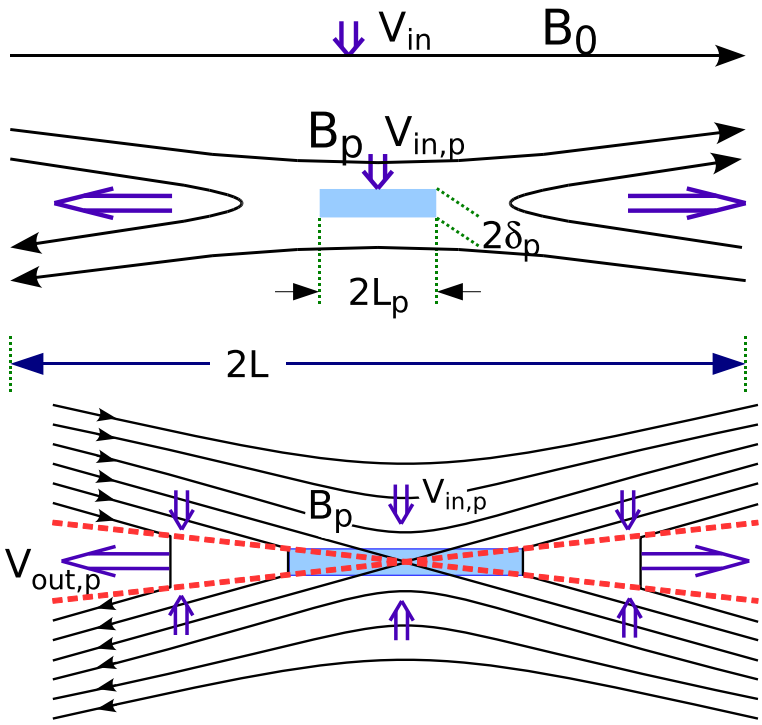

Figure 7.3: Illustration of the Petschek reconnection geometry. Top: Scales assumed in Petschek's model; Bottom: illustration of the diffusion region and the attached slow shocks.

Figure 7.3 illustrates the basic reconnection geometry that Petschek suggested. The main point in Petschek's model is that the length of the diffusion region should be much shorter $L_p \ll L$ in order to realize a higher reconnection rate. The basic scaling in his model is illustrated in Figure 7.3. Note that a much shorter diffusion region also implies a thinner diffusion region, i.e., $\delta_p \ll \delta$, because faster reconnection implies a larger electric field and therefore also a higher current density at the x-line. The fast transport out of this diffusion region over the scale from L_p to L occurs through a flow layer which is bounded by slow shocks.

Let us first look at the scaling in the vicinity of the diffusion region. The magnetic field in the inflow of the Petschek region is denoted B_p which is smaller than B_0. However, since we have magnetic flux conservation $v_{in}B_0 = v_{in,p}B_p$ (and assuming constant mass density) the inflow Alfven Mach number relate with $v_{A,p} = B_p/\sqrt{\mu_0\rho} = v_A B_p/B_0$ as

$$\frac{M_{in}}{M_{in,p}} = \frac{v_{in}}{v_{in,p}}\frac{v_{A,p}}{v_A} = \frac{B_p^2}{B_0^2}$$

For the length scale we obtain with $R = \mu_0 L v_A/\eta$ and $R_p = \mu_0 L_p v_{A,p}/\eta$ and using $R_p = v_{A,p}^2/v_{in,p}^2 = 1/M_{in,p}^2$

$$\frac{L_p}{L} = \frac{R_p}{R}\frac{v_A}{v_{A,p}} = \frac{1}{R}\frac{v_A}{v_{A,p}}\frac{v_{A,p}^2}{v_{in,p}^2} = \frac{1}{R}\frac{v_{A,p}^2}{v_{in,p}^2}\frac{B_0}{B_p}$$

with $B_0/B_p = M_{in,p}^{1/2}/M_{in}^{1/2}$ we obtain

$$\frac{L_p}{L} = \frac{1}{R}\frac{1}{M_{in,p}^{3/2}}\frac{1}{M_{in}^{1/2}}$$

and

$$\frac{\delta_p}{L} = \frac{L_p}{L}\frac{1}{\sqrt{R_p}} = \frac{1}{R}\frac{1}{M_{in,p}^{3/2}}\frac{1}{M_{in}^{1/2}}M_{in,p} = \frac{1}{R}\frac{1}{M_{in}^{1/2}}\frac{1}{M_{in,p}^{1/2}}$$

Thus, once we have determined B_p/B_0 we can obtain the ratio of the inflow Mach numbers as well as the scale of the Petschek diffusion region. Note that this is really just a re-scaling of the diffusion region in size and is applicable to any smaller scale diffusion region. It should also be remarked that similar to the Sweet-Parker model, this model of reconnection does not treat the diffusion region self-consistently.

The main insight from Petschek was that the the transport from L_p to L does not require the thin outflow layer. Petschek suggested that the outflow region is bounded by two slow switch-off shocks (thick red lines in Figure 7.3). Note that this is strictly only true if the shocks are horizontal, i.e., aligned with the z direction. However, since the shocks are only very slightly inclined the error in the assumption of switch-off shocks is small. From the discussion of switch-off slow shocks we know that in the de-Hoffmann-Teller frame (in which the flow is field-aligned) the upstream velocity is $u_u = v_{Au}$ (equation 6.84) such that the tangential and normal components of the upstream velocity are

$$\begin{aligned} u_{tu} &= \frac{B_{tu}}{\sqrt{\mu_0\rho_u}} = v_{At} \\ u_{nu} &= \frac{B_n}{\sqrt{\mu_0\rho_u}} = v_{An} \end{aligned}$$

However, the rest frame of the diffusion region is not the de-Hoffmann-Teller (dHT) frame. In the rest frame the flow is almost normal to the shock. Therefore the transformation into the dHT frame requires to add a velocity of $u_t = v_{At}$ to the rest frame. In other words the plasma in the outflow region must be jetting at the speed of

$$v_{out,p} = v_{At,p} \approx B_p/\sqrt{\mu_0\rho}$$

away from the diffusion region to satisfy the switch-off shock conditions. Secondly it should be noted that the actual normal velocity in the downstream (outflow) region is 0. This means that the slow shock is moving with a velocity u_{nu} toward the upstream (inflow) region.

The prior discussion assumes that the density is constant, which is incorrect for a slow shock. In fact we can compute the outflow density from the switch-off shock properties. To do so one has to determine the angle of the upstream magnetic field with the shock normal. The tangential component of this field is B_p and the normal component is B_n. Magnetic flux conservation implies $v_{nu}B_p = v_{At,p}B_n$ such that

$$\tan\theta = \frac{B_n}{B_p} = \frac{v_{nu}}{v_{At,p}} = r_p$$

where r_p is the reconnection rate for the Petschek diffusion region. This illustrates that $\theta \approx r_p \ll 1$ such that the compression is approximately $X = 1 + \left(2c_s^2/v_{A,p}^2 + \gamma - 1\right)^{-1}$. The resulting maximum compression occurs for $c_s^2 \ll v_{A,p}^2$ with $X = 5/2$. This result can be utilized to correct the Sweet-Parker discussion of the diffusion region for different in- and outflow densities. Using mass conservation the Sweet-Parker reconnection rate is corrected to

$$\frac{v_{in}}{v_A} = \left(\frac{\rho_{out}}{\rho_{in}}\right)^{1/4}\left(\frac{\eta}{\mu_0 L v_A}\right)^{1/2} = \left(\frac{\rho_{out}}{\rho_{in}}\right)^{1/4}\frac{1}{\sqrt{R}}$$

(e.g. Priest, 2000) such that the actual change in the reconnection rate is rather small and we can ignore this correction for the Petschek mechanism.

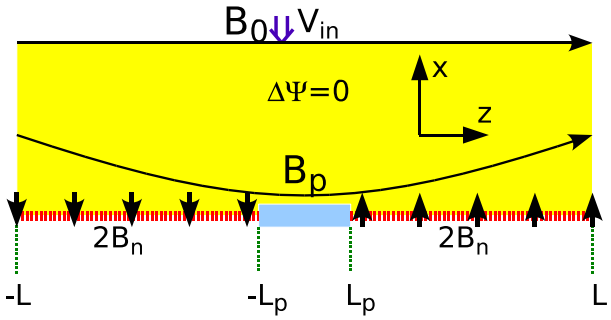

Figure 7.4: Sketch of the inflow field solution in Petschek's model.

Finally it is important to determined the magnetic field at the diffusion region B_p. This field is modified because the field in the vicinity of the diffusion region is curved and different from the field B_0 at large distance from the diffusion region (Figure 7.4). The field perturbation $\mathbf{B}_c$ in the inflow region is assumed to by derived from a potential Ψ (such that $\nabla \times \mathbf{B}_c = 0$). At the slow shocks the magnetic field should be B_n, however, here the shocks have an inclination of $\delta_p/L_p = v_{in,p}/v_{A,t} = B_n/B_p$ with the z axis. To account for this we actually need a boundary value of $2B_n$ for the magnetic field correction in the inflow region from $-L$ to $-L_p$ and from L_p to L along the z axis. Projected onto the slow shock with the inclination B_n/B_p this yields a normal magnetic field of B_n. Assuming that the field is generated from a continuous series of monopoles along the shocks (red line in Figure 7.4, the field correction from the monopoles observed at $\mathbf{r}_0$ from a line element dz at $\mathbf{r} = (0, z)$ is then

$$d\mathbf{B}_c = \frac{2B_n\left(\mathbf{r}_0 - \mathbf{r}\right)}{\pi\left(\mathbf{r}_0 - \mathbf{r}\right)^2}dz$$

The total field correction is obtained by integrating along the z axis

$$\mathbf{B}_c = \frac{2B_n}{\pi}\left(-\int_{-L}^{-L_p}\frac{(\mathbf{r}_0-\mathbf{r})\,dz}{|\mathbf{r}_0-\mathbf{r}|^2}+\int_{L_p}^{L}\frac{(\mathbf{r}_0-\mathbf{r})\,dz}{|\mathbf{r}_0-\mathbf{r}|^2}\right)$$

where the minus sign in the first term is to generate $-2B_n$ for $z<0$. To illustrates this let us take as an example a sheet of monopoles from $-d$ to $+d$ along the z axis. The x component (normal) of the field observed at $\mathbf{r}_0=(x_0,z_0)$is

$$\begin{aligned} B_x(x_0,z_0) &= \frac{2B_n}{\pi}\left(\int_{-d}^{d}\frac{x_0 dz}{|\mathbf{r}_0-\mathbf{r}|^2}\right)=\frac{2B_n}{\pi}x_0\left(\int_{-d}^{d}\frac{dz}{x_0^2+(z_0-z)^2}\right)\\ &= \frac{2B_n}{\pi}x_0\left(\int_{-d-z_0}^{d-z_0}\frac{d\widetilde{z}}{x_0^2+\widetilde{z}^2}\right)=\frac{2B_n}{\pi}x_0\frac{1}{x_0}\left(\arctan\frac{d-z_0}{x_0}-\arctan\frac{-d-z_0}{x_0}\right)\end{aligned}$$

Considering the limit $x_0\to 0$ for $-d<z_0<d$ yields $B_x(0,z_0)=2B_n$ as expected. Using now the monopole distribution of Figure 7.4 and computing the z component in the center of the diffusion region yields the desired correction to the magnetic field in the inflow region:

$$\begin{aligned} B_{z,c}(x,z=0) &= \frac{2B_n}{\pi}\left(\int_{-L}^{-L_p}\frac{dz}{z}-\int_{L_p}^{L}\frac{dz}{z}\right)\\ &= \frac{2B_n}{\pi}\left(\ln\frac{L_p}{L}-\ln\frac{L}{L_p}\right)=-\frac{4B_n}{\pi}\ln\frac{L}{L_p}\end{aligned}$$

Adding this field to the homogeneous field yields the magnetic field at the diffusion region

$$B_p = B_0-\frac{4B_n}{\pi}\ln\frac{L}{L_p}=B_0\left(1-\frac{4M_{in}}{\pi}\ln\frac{L}{L_p}\right)$$

For $\frac{4M_{in}}{\pi}\ln\frac{L}{L_p}\le 1/2$ the above expression implies $B_p\approx B_0$ such that $M_{in,p}\approx M_{in}$ and the relations for the diffusion region scales become

$$\frac{L_p}{L}=\frac{1}{R}\frac{1}{M_{in}^2}\qquad \frac{\delta_p}{L}=\frac{1}{R}\frac{1}{M_{in}}$$

Petschek suggested that the process becomes inefficient if B_p becomes too small. Assuming that a reasonable value for the minimum B_p is $B_p\approx B_0/2$ yields for the approximate maximum inflow Mach number (or reconnection rate)

$$M_{in}=r_p\approx\frac{\pi}{8\ln(L/L_p)}=\frac{\pi}{8\ln(M_{in}^2R)}\approx\frac{\pi}{8\ln R}$$

This reconnection rate is much larger than the Sweet-Parker rate. For instance for a Lundquist number of $R=10^8$ the Petschek reconnection rate is $r_p\approx 2\cdot 10^{-2}$ compared to a Sweet-Parker rate of

$r_{sp} \approx 10^{-4}$. The reason is as stated that the aspect ratio δ_p/L_p is much larger than δ/L for the Sweet-Parker diffusion region. This is accomplished by a much smaller length of the diffusion region $L_p \approx L64\ln^2 R/\left(\pi^2 R\right)$. However, it is also important to note that the thickness of the Petschek diffusion region is much smaller $\delta_p \approx \delta 8 \ln R/\left(\pi\sqrt{R}\right)$. This is required because the larger reconnection rate must be equivalent to a larger electric field $E_{xl} = \eta j_{xl} = \eta B_p/\left(\mu_0 \delta_p\right)$ which requires a $\delta_p \ll \delta$. This concept of reconnection is remarkably simple and it was able to explain many observations in terms of magnetic reconnection where the Sweet-Parker rate was far too small.

Another important aspect is the near scale invariance of Petschek reconnection. If the inflow magnetic field $B_0$and density ρ_0 are given, the Sweet-Parker range obviously depends on the scale L. However, since the Petschek rate depends only on $\ln R$, it various only between 0.09 and 0.01 for Lundquist numbers ranging from 10^2 to 10^{20} such that a value of $r_p \approx 3 \cdot 10^{-2}$ is a reasonable representation for most plasmas. With Ohm's law this also implies that $\delta_p \approx \eta/\left(\mu_0 r_p v_A\right)$ which is fairly insensitive to the macroscopic length scale L.

7.5 Application and Further Discussion of Magnetic Reconnection

7.5.1 Diffusion and Reconnection Parameters or the Giant Sliced by a String

Magnetic reconnection is important in many different space plasma systems. A key issue for reconnection models are their properties applied to particular systems and how these compare to actual observations. The following table lists various typical parameters for diffusion, Sweet-Parker reconnection and Petschek reconnection applied to the magnetopause, the magnetotail, and flares in the solar corona.

	Magnetopause	Magnetotail	Solar corona (flares)
n_0 [cm^{-3}]	4	0.5	$6 \cdot 10^8$
B_0 [nT]	40	20	$3 \cdot 10^7$
L [m]	10^6	10^7	10^7
v_A [m/s]	$4.4 \cdot 10^5$	$6.2 \cdot 10^5$	$2.7 \cdot 10^7$
$E_0 = v_A B_0$ [V]	$1.8 \cdot 10^{-2}$	$1.3 \cdot 10^{-2}$	$8 \cdot 10^5$
τ_A $[s]$	2.3	1.6	0.37
v_{thi} $[K]$	10^5	$7 \cdot 10^5$	10^5
v_{the} $[K]$	$1.3 \cdot 10^6$	10^7	$4.3 \cdot 10^6$
λ_e [m]	$2.7 \cdot 10^3$	$8.0 \cdot 10^3$	0.2
τ_{diff} $[s]$	$7 \cdot 10^{11}$	$1.5 \cdot 10^{15}$	$2.5 \cdot 10^{14}$
R	$3 \cdot 10^{11}$	10^{15}	10^{15}
r_{sp}	$1.8 \cdot 10^{-6}$	$3 \cdot 10^{-8}$	$3 \cdot 10^{-8}$
r_p	$1.5 \cdot 10^{-2}$	$1.1 \cdot 10^{-2}$	$1.1 \cdot 10^{-2}$
r_{obs}	$3 \cdot 10^{-2}$	$3 \cdot 10^{-2}$	$10^{-4}$to 10^{-2}
δ_{sp} [m]	1.8	0.3	0.3
δ_p [m]	$2 \cdot 10^{-4}$	10^{-6}	10^{-6}
L_p [m]	$1.4 \cdot 10^{-2}$	10^{-4}	10^{-4}

The table demonstrates that particularly the values for the observed reconnection rates are much more realistic for the Petschek model. However, it also illustrates that the dimensions of the Petschek diffusion region are awfully small based on Coulomb collisions. We will return to this issue in a moment. In fact when considering the gigantic scales of magnetospheric or solar magnetic field of ten thousands of km and assuming that these field are reconnected on a potential fast time scale in a region that has some 10^{-6} to 10^{-2} m in size is difficult to imagine. However before we attend to this problem in more detail let us look at some other properties.

The next table shows typical time scales and velocities associated with diffusion, Sweet-Parker and Petschek reconnection. Here velocities refer to the inflow velocity and the time scales denote the time needed to reconnect magnetic flux in a layer of thickness L. Again the table illustrates that times for diffusion and Sweet-Parker reconnection are extremely long and the corresponding velocities are unrealistically small. Vice versa Petschek reconnection appears to produce realistic times and reconnection velocities for all three systems.

	Magnetopause	Magnetotail	Solar corona (flares)
L [m]	10^6	10^7	10^7
v_A [m/s]	$4.4 \cdot 10^5$	$6.2 \cdot 10^5$	$2.7 \cdot 10^7$
τ_A $[s]$	2.3	1.6	0.37
R	$3 \cdot 10^{11}$	10^{15}	10^{15}
τ_{diff} $[s]$	$7 \cdot 10^{11}$	$1.5 \cdot 10^{15}$	$2.5 \cdot 10^{14}$
τ_{sp} $[s]$	10^6	$5 \cdot 10^7$	10^7
τ_p $[s]$	150	150	35
v_{diff} [m/s]	$1.5 \cdot 10^{-6}$	$6 \cdot 10^{-10}$	$2.7 \cdot 10^{-8}$
v_{sp} [m/s]	0.8	0.02	0.1
v_p [m/s]	$3 \cdot 10^3$	$5.5 \cdot 10^3$	$2.5 \cdot 10^5$

7.5.2 Diffusion Region Physics - Anomalous Resistivity or a Bigger String

There have been many attempts to improve Petschek's reconnection [*Valyliunas*, 1975; *Priest and Forbes*, 2000], however, there is to-date no self-consistent treatment off the diffusion region. We pointed out one possible problem in the different dynamics of continuity and pressure equation. A much discussed topic is the length of the diffusion region. Petschek argued that the diffusion region adjusts in order to realize a large reconnection rate. However, for constant resistivity many numerical simulation and some analytic estimates indicate that in the opposite, an initially short diffusion rate may in fact lengthen and lead to a lower reconnection rate approach the Sweet-Parker rate as time continues. Another issue with the application of both, Sweet-Parker and Petschek reconnection is the width of the diffusion region. The above table illustrates that this is of the order of meters for the considered applications for Sweet-Parker reconnection and of the order of 10^{-4} to 10^{-6}m for Petschek reconnection. Clearly there seems to be something odd about this. To shed more light on this issue let us compute the drift speed that is necessary to maintain the current for Sweet-Parker reconnection.

$$j \;=\; ne\,(v_{di} - v_{de}) = \frac{B_0}{\mu_0 \delta} \quad or$$

$$v_{di} - v_{de} = \frac{B_0}{\mu_0 ne\delta} = \frac{B_0}{\sqrt{\mu_0 m_i n}} \frac{c\left(\epsilon_0 m_i\right)^{1/2}}{\left(\mu_0 ne^2\right)^{1/2}\delta} = v_A \frac{c}{\omega_{pi}\delta}$$

In other words $v_{di} - v_{de} = v_A \lambda_i/\delta$. Here $\lambda_i = \lambda_e\sqrt{m_i/m_e}$ is the ion inertial length which is 100 km, 400 km, and 10 m for the magnetopause, the magnetotail, and the solar corona respectively. his illustrates that the relative drift speed approaches the Alfvén speed when the diffusion region width becomes the ion inertial length. Clearly the Sweet-Parker and the Petschek diffusion region widths based on Coulomb collisions are already much thinner then λ_i such that the current drift speed exceed the Alfvén speed by orders of magnitude. We gain still more insight by comparing the drift speed with the ion thermal velocity.

$$\frac{v_{di} - v_{de}}{v_{thi}} = \frac{v_A}{v_{thi}} \frac{\lambda_i}{\delta}$$

The current drift speed equals the ion thermal speed for

$$\delta = \delta_i = \frac{\lambda_i v_A}{v_{thi}}$$

The significance of this is that current sheets thinner then δ_i implies drift speeds in excess of the ion thermal speed can be expected to generate micro-instabilities. The turbulent interaction of the waves with the current carrying particles will slow the particle to conditions sub-critical for the instability. Typical instabilities discussed in this context are the lower hybrid drift instability, the ion acoustic instability, the modified two-stream (Buneman) instability, and ion or electron cyclotron waves. The precise onset conditions for these instabilities vary and depend on the magnetic field and plasma configuration. The actual onset of the instabilities requires often a somewhat higher drift speed, foe instance the ion acoustic instability either requires a significantly higher drift speed or a much higher electron temperature. A reasonable minimum requirement for the onset of strong turbulence through micro-instabilities could require the drift speed to exceed the electron thermal velocity

$$\frac{v_{di} - v_{de}}{v_{the}} = \frac{v_A}{v_{the}} \frac{\lambda_i}{\delta}$$

which yields the condition for onset

$$\delta = \delta_e = \frac{\lambda_i v_A}{v_{the}}$$

We can now use the results for Sweet-Parker and Petschek reconnection to infer the necessary Lundquist number and the collision frequency. With $R = \tau_{diff}/\tau_A = L^2/(\lambda_e^2 \nu_c \tau_A)$ Sweet parker reconnection yields

$$\frac{\delta}{L} = \frac{1}{\sqrt{R}} = \frac{\lambda_e}{L}\sqrt{\nu_{sp}\tau_A}$$

Using the current constraints δ_i and δ_e and solving for the required collision frequencies yields

$$\nu_{sp,i} = \frac{m_i v_A^2}{\tau_A m_e v_{thi}^2} \quad \text{and} \quad \nu_{sp,e} = \frac{m_i v_A^2}{\tau_A m_e v_{the}^2}$$

for the frequencies corresponding to δ_i and δ_e respectively. Using $\delta/L = R^{-1/2}$ and solving for the Lundquist numbers yields

$$R_{sp,i} = \frac{L^2}{\lambda_i^2}\frac{v_{thi}^2}{v_A^2} \quad \text{and} \quad R_{sp,e} = \frac{L^2}{\lambda_i^2}\frac{v_{the}^2}{v_A^2}$$

For Petschek reconnection $\delta_p/L = 1/(rR)$ and $R = \tau_{diff}/\tau_A = L^2/(\lambda_e^2 \nu_c \tau_A)$ with the constraints δ_i and $\delta_e$we have

$$\frac{1}{rR} = \frac{\lambda_i v_A}{L v_{thi}} \quad \text{or} \quad = \frac{\lambda_i v_A}{L v_{the}}$$

Solving for the required anomalous collision frequency

$$\nu_{p,i} = r\frac{\lambda_i v_A^2}{\lambda_e^2 v_{thi}} \quad \text{and} \quad \nu_{p,e} = r\frac{\lambda_i v_A^2}{\lambda_e^2 v_{the}}$$

corresponding to δ_i and δ_e respectively. Similarly the Lundquist numbers for the current constraints and Petschek reconnection are

$$R_{p,i} = \frac{1}{r}\frac{L v_{thi}}{\lambda_i v_A} \quad \text{and} \quad R_{p,e} = \frac{1}{r}\frac{L v_{the}}{\lambda_i v_A}$$

Results for these reconnection parameters assuming a current limitation are given in the following table.

	Magnetopause	Magnetotail	Solar corona (flares)
L [m]	10^6	10^7	10^7
v_A [m/s]	$4.4 \cdot 10^5$	$6.2 \cdot 10^5$	$2.7 \cdot 10^7$
τ_A $[s]$	2.3	1.6	0.37
v_{thi} $[K]$	10^5	$6.2 \cdot 10^5$	10^5
v_{the} $[K]$	$1.3 \cdot 10^6$	10^7	$4.3 \cdot 10^6$
λ_i [m]	$1.2 \cdot 10^5$	$3.4 \cdot 10^5$	8.6
λ_e [m]	$2.7 \cdot 10^3$	$8.0 \cdot 10^3$	0.2
δ_i [m]	$5.3 \cdot 10^5$	$3.4 \cdot 10^5$	$2.3 \cdot 10^3$
δ_e [m]	$4.1 \cdot 10^4$	$2.1 \cdot 10^4$	54
L/λ_i	8.3	29	$1.2 \cdot 10^6$
L^2/λ_i^2	69	870	$1.4 \cdot 10^{12}$
L^2/λ_e^2	$1.4 \cdot 10^5$	$1.6 \cdot 10^6$	$2.5 \cdot 10^{15}$
$R_{sp,i}$	3.6	870	$1.9 \cdot 10^7$
$R_{sp,e}$	600	$2.3 \cdot 10^5$	$3.6 \cdot 10^{10}$
$\nu_{sp,i}$ $[s^{-1}]$	$1.5 \cdot 10^4$	$1.1 \cdot 10^3$	$5.0 \cdot 10^7$
$\nu_{sp,e}$ $[s^{-1}]$	91	4.4	$2.0 \cdot 10^5$
τ_{diff} $[s]$	$7 \cdot 10^{11}$	$1.5 \cdot 10^{15}$	$2.5 \cdot 10^{14}$
$R_{p,i}$	14	410	$6.3 \cdot 10^6$
$R_{p,e}$	360	$9.4 \cdot 10^3$	$4.1 \cdot 10^8$
$\nu_{p,i}$ $[s^{-1}]$	320	$3.4 \cdot 10^3$	$3.6 \cdot 10^9$
$\nu_{p,e}$ $[s^{-1}]$	24	210	$8.3 \cdot 10^7$
$L^2/\left(\lambda_e^2 \tau_A\right)$	$6.1 \cdot 10^4$	10^6	$6.8 \cdot 10^{15}$
$r_{sp,i}$	0.8	$6 \cdot 10^{-2}$	$7 \cdot 10^{-4}$
$r_{sp,e}$	$6 \cdot 10^{-2}$	$1.5 \cdot 10^{-2}$	$1.1 \cdot 10^{-4}$
$r_{p,i}$	0.13	$7 \cdot 10^{-2}$	$3 \cdot 10^{-2}$
$r_{p,e}$	$7 \cdot 10^{-2}$	$5 \cdot 10^{-2}$	$2 \cdot 10^{-2}$

The derived parameters shed much light on the physics needed to maintain either the Sweet-Parker of the Petschek reconnection geometry. The basic idea behind these parameters is rather simple in that it is assumed that the current width of the diffusion region cannot collapse below a meaningful physical length scale. The criterion applied uses a current limitation based on the generation of strong turbulence which is assumed to inhibit any further reduction in the width of the current in the diffusion region.

Since the limiting width scales with λ_i, it is not surprising that the Lundquist numbers for the different cases involve the factor L/λ_i. I should also be noted that the required collision frequencies for Sweet-Parker reconnection are not scale independent but are proportional to $1/\tau_A = v_A/L$. In contrast the collision frequencies for Petschek reconnection are indeed mostly independent of L (there is a weak logarithmic dependence through the actual reconnection rate r). In other words, if reconnection occurs on a fast time scale and the diffusion region width is limited by the current that can flow through the region, the required anomalous collision frequencies are fixed within a certain range (depending on the details of the current limitation).

Considering the values in the above table a number of properties are noteworthy: The current limitation anomalous collision frequencies many orders of magnitude higher then the actual coulomb collision frequencies. For the magnetopause and the magnetotail the resulting reconnection rates of

Sweet-Parker reconnection and Petschek reconnection are fairly comparable. The reason for this is that for these current systems the macroscopic scale is only one or two orders of magnitude larger then the current limitation scale δ_i or δ_e. It should be remarked that for the magnetosphere the scale $\delta_e$is probably the more relevant scale because the onset condition for micro-instabilities is usually closer to the electron thermal speed. It should also be remarked that reconnection rates close to 1 are unrealistic. They would imply that the aspect ratio is close to one which implies a separatrix angle of 45°. However, for such an angle the magnetic field at the X-line can be constructed from a vacuum field, i.e., there is no or very little current at the X-line at which point reconnection must switch of. In summary, the current limitation leads to more realistic scale of the diffusion region but it is still impressive that regions of the size of a few 10 meters (for the corona) or a few 10 km (magnetosphere) can generate all the reconnection that is need in very large scale system to reconnect a major amount of the magnetic flux in the system.

7.5.3 Diffusion Region Physics - Length of the Diffusion Region

In terms of the observations it is not clear that reconnection occurs everywhere on a fast Petschek-like rate. However, there is clear evidence that reconnection particularly in the magnetosphere does often occur with a fast reconnection rate.

This previous section poses some fundamental new questions. Most strikingly the current limitation does not provide a unique answer to the actual collision frequency. This is clearly demonstrated for the solar applications. Here the current limitation applied to Sweet-Parker and Petschek reconnection uses the same width but yields different anomalous collision frequencies, Lundquist numbers, and reconnection rates. The basic difference here is the length of the assumed diffusion region. The long Sweet-Parker diffusion region leads to a much slower diffusion-like process for the same current width as the shorter Petschek diffusion region. This poses the question as to what determines the length of the diffusion region? There has been much research on this point which examines these processes often in relation to particular in- and outflow boundary conditions.

While this work sheds some important new light on reconnection it is not clear, how particular boundary conditions can be applied to a reconnection process at the magnetopause or the sun where diffusion regions of reconnection occupy only a minute fraction of the overall volume.

There are several aspects of recent research that are important important for the physics of the diffusion region. So far the discussion had assumed that the resistivity is constant and numerical simulation in deed support the result that the diffusion region tends to lengthen in simulations even if it is initially set up to be short to support Petschek-type reconnection. However, if the resistivity is caused by turbulence the assumption of constant resistivity is not anymore correct. Since the turbulence is driven by the strength of the current density the resistivity becomes current dependent. This in fact has shown the result in simulations that the diffusion region stays much shorter and reconnection is fast as suggested by Petschek.

In recent year there has been a new development in that the inclusion of the Hall term appears to have a strong influence on reconnection. In fact it was found in a simple numerical reconnection experiment that different plasma approximation (Hall MHD, Two-fluid plasma, Hybrid simulations with ions as particles and electrons as fluid, and full particle simulations) all show approximately the same fast reconnection rate[*Birn et al.*, 2001; *Otto*, 2001; *Shay et al.*, 2001]. While details in the reconnection geometry were different in these simulations they all showed a short diffusion region (few ion inertia lengths) and a width that was some fraction of ion inertial length. This finding was in contrast to

pure MHD models where the diffusion region tended to lengthen with a lower reconnection rate. The common physics in all models with fast Petschek-like reconnection was the inclusion of Hall Physics.

The physics of the diffusion region including the Hall term in Ohm's law is more complicated. One of the most important aspects is that the frozen-in condition now applies to the electrons in the plasma. The electrons also carry much of the current in the diffusion region and are moving into the y direction (into the plane in 2D reconnection) So, during their acceleration out of the diffusion region they not only move along z but also in y. Since the magnetic field is moving with the electrons magnetic field lines in the symmetry plane ($x = 0$) now are displaced (bent) along y which means that different from MHD now there are in- and out-of plane magnetic field and flow components. This rotation of the magnetic field is known for whistler wave and whistler wave are in fact facilitated through the inclusion of the Hall term. So the build up of a very characteristic pattern of B_y magnetic field is typical for Hall reconnection. However, this in turn provides another argument for the limitation of the length of the diffusion region. If the diffusion region were long and thin the current density would be high of a large distance along the diffusion region. This would generate very strong B_y flux over an extended region along the diffusion region. However, this generation requires energy and allows that the process can operate only of a limited length thereby providing a limitation of the length of the diffusion region.

Finally it should be noted that there are still other aspects that can play a role. Simulations indicate that the other terms in general Ohm's law can contribute to the reconnection electric field. Specifically the electron pressure tensor and the electron inertial term. Currently there is no final conclusion regarding these problems of the physics of the diffusion region. This is in part also because the real world is three-dimensional which contributes additional complication and becomes a computational challenge particularly for particle simulations. It not unlikely that there is no unique answer to the reconnection problem and that it really depends on the specific plasma parameters and the geometry of the current layers. For instance it is well known and easy to demonstrate the plasma flow in the inflow regions can alter the reconnection rate and structure of the reconnection geometry. For instance if flow along the magnetic field in the inflow regions surpasses the Alfvén speed reconnection must shut off. The information that reconnection operates is transmitted at Alfvén speed and if the plasma in the inflow region is jetting faster this information cannot spread such the reconnection is switched-off.

Fortunately for many applications of reconnection, the details of the diffusion region may not matter too much as long as a model approximates the reconnection rate sufficiently well. Since the diffusion region occupies only a tiny volume of the overall configuration, all large scale feature such as mass, momentum, energy, and magnetic flux transport are reasonably approximated if a uses a good approximate too the reconnection rate independent of details in the diffusion region.